

# Electronic Supplementary Information

For

## **Slow Deactivation Channels in UV-Photoexcited Adenine DNA**

*Xuebo Chen<sup>a</sup>, Weihai Fang<sup>a</sup>, and Haobin Wang<sup>b</sup>*

*<sup>a</sup>Key Laboratory of Theoretical and Computational Photochemistry of Ministry of Education,  
Department of Chemistry, Beijing Normal University, Xin-wai-da-jie No. 19, Beijing, 100875, People's  
Republic of China*

*<sup>b</sup>Department of Chemistry and Biochemistry, New Mexico State University, Las Cruces, NM 88003,  
USA*

## Contents

Page no.

1. Section 1. Vertical excitation for the adenine monomer and the aqueous (dA)<sub>5</sub> .....S3~S3
2. Section 2. The relaxation paths in the S<sub>N3P</sub>(<sup>1</sup>nπ\*) and S<sub>N7P</sub>(<sup>1</sup>nπ\*) states.....S4~S9
3. Section 3. Computational details ..... S10~S14
4. Section 4. Tables..... S15~S26
5. Section5 . Energy tables and cartesian coordinates of the optimized structures..... S27

**Section 1.** Vertical excitation for the adenine monomer and the aqueous (dA)<sub>5</sub>

**Table S1.** Vertical ( $E_{\perp}$ , eV) excitation energies, oscillator strengths ( $f$ ), dipole moments (D.M., Debye), and state characterizations at the Franck-Condon for the adenine monomer (A) in vacuo and the (dA)<sub>5</sub> oligomer in a water solvent box. The values in italic for aqueous d(A)<sub>5</sub> were taken from CAS(14e/10o)/Amber ground state optimizations following by eight roots state average CASPT2 computations and the rest values for vertical excitation of d(A)<sub>5</sub> were taken from CAS(14e/10o)/Amber ground state optimizations following by seven roots state average CASPT2 calculations.

Transitions	A in vacuo			aqueous (dA) <sub>5</sub> (A dimer in QM subsystem)		
	$f$	$E_{\perp}$	D.M.	$f$	$E_{\perp}$	D.M.
S <sub>0</sub>	--	0.0	2.48	--	0.0	4.60
S <sub>0</sub> →S <sub>N1P</sub> ( <sup>1</sup> nπ*)	0.0014	4.80	1.19	0.140	4.91	4.87
S <sub>0</sub> →S <sub>N3P</sub> ( <sup>1</sup> nπ*)	0.0071	5.96	0.75	0.0195	5.34	5.38
S <sub>0</sub> →S <sub>N7P</sub> ( <sup>1</sup> nπ*)	0.016	6.29	3.07	<i>0.0161</i>	<i>6.06</i>	<i>3.27</i>
S <sub>0</sub> →S <sub>Lb</sub> ( <sup>1</sup> ππ*)	0.046	4.94	2.40	0.0411	5.26	4.33
S <sub>0</sub> →S <sub>La</sub> ( <sup>1</sup> ππ*)	0.289	5.53	4.57	--	--	--
S <sub>0</sub> →S <sub>stack1</sub> ( <sup>1</sup> ππ*)	--	--	--	0.714(0.36)	5.24	6.93
S <sub>0</sub> →S <sub>stack2</sub> ( <sup>1</sup> ππ*)	--	--	--	0.215	4.84	5.28
S <sub>0</sub> →S <sub>CT</sub> ( <sup>1</sup> ππ*)	--	--	--	0.0119	6.31	14.81

## Section 2. The relaxation paths in the $S_{N3P}(^1n\pi^*)$ and $S_{N7P}(^1n\pi^*)$ states.

The relaxation paths of the other two  $n \rightarrow \pi^*$  transitions for the adenine monomer and aqueous  $(dA)_5$ , originated from promoting lone pair electron of N3 [ $S_{N3P}(^1n\pi^*)$ ], and N7 [ $S_{N7P}(^1n\pi^*)$ ] atoms, were also examined in Figures S1 and Figure S2. The vertical excitation energy of  $S_0 \rightarrow S_{N1P}(^1n\pi^*)$  transition increases from 4.80 eV for the adenine monomer to 4.91 eV for the aqueous  $d(A)_5$  due to the effect of base stacking. In contrast, the vertical excitation energies of  $S_0 \rightarrow S_{N3P}(^1n\pi^*)$  and  $S_0 \rightarrow S_{N7P}(^1n\pi^*)$  transitions for the aqueous  $d(A)_5$  are respectively 0.62 and 0.23 eV red-shifted with respect to those of the adenine monomer in vacuo. This indicates that base stacking exerts negligible influences on the  $S_0 \rightarrow S_{N3P}(^1n\pi^*)$  and  $S_0 \rightarrow S_{N7P}(^1n\pi^*)$  excitations and participation of water molecules may play important roles on the red-shifted energy levels of vertical excitations. It is generally accepted that water molecule may impose a polar environment and hydrogen bonds through  $H_2N \cdots H-OH$  or  $C=O \cdots H-OH$  models. One does not expect that a polar environment cause significant influence on the  $n \rightarrow \pi^*$  transition since it leads to the diradical configuration. However, the formation of hydrogen bond was found to result in the improvement of  $n \rightarrow \pi^*$  vertical excitation energies about 0.18 ~ 0.43 eV due to the unfavorable influence of mutual attraction on the electron promotion of the lone pair.<sup>S1, S2</sup> Since  $n \rightarrow \pi^*$  transition excitation energy is not the focus of this work and the use of model hydrogen bond complex unnecessarily complicates the understanding to the photophysics of UV-irradiated DNA, hydrogen bond is not considered in the present

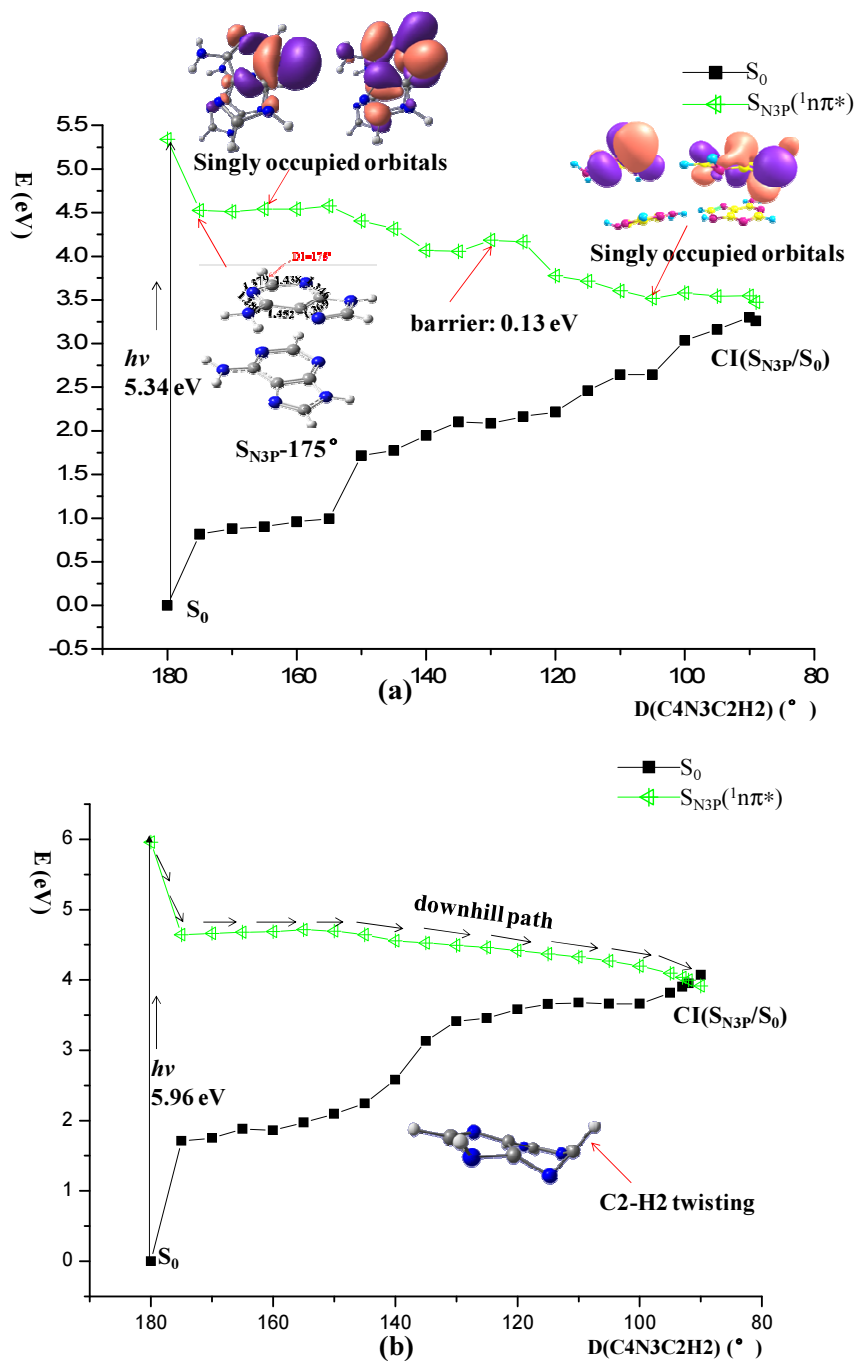


Figure S1. Illustrative relaxation path for the ground state recovery of (a) an aqueous  $(dA)_5$ ; and (b) an adenine monomer in the gas phase; starting from the FC point of the  $S_{N3P}(^1n\pi^*)$  state along the RC defined by dihedral angle  $C4N3C2H2$ .

work. The decay of the  $S_{N3P}(^1n\pi^*)$  state through the structural deformation of the C2-H2 bond twisting is shown in Figure S1 (a). With increased dihedral angle C4N3C2H2, the singly occupied orbitals gradually shows some CT  $\pi \rightarrow \pi^*$  transition character, which is sensitive to the polarity of the water solvent. This is another reason why a relative large red-shifted vertical excitation energy of the  $S_0 \rightarrow S_{N3P}(^1n\pi^*)$  transition is found from adenine monomer in vacuo to aqueous  $(dA)_5$ . It also explains the dipole moment change ( $\Delta=1.27$  Debye) in FC region as compared with that of  $S_0 \rightarrow S_{N1P}(^1n\pi^*)$  ( $\Delta=0.27$  Debye). Keeping in mind that the previous computational and experimental studies are mostly concentrated on the lowest lying  $S_0 \rightarrow S_{N1P}(^1n\pi^*)$  excitation, the differentiation of all the possible  $n \rightarrow \pi^*$  transition patterns in this work will facilitate a better understanding of the complicated excited state dynamics of DNA.

Figures S1 and S2 illustrate respectively the relaxation paths in the  $S_{N3P}(^1n\pi^*)$  and  $S_{N7P}(^1n\pi^*)$  states for the aqueous  $(dA)_5$  and adenine monomer in the gas phase. The first  $n \rightarrow \pi^*$  transition corresponds to the lone pair of the N3 atom and the anti-bonding  $\pi^*$  orbital mainly localized in the six-membered ring, whereas the second corresponds to the lone pair of the N7 atom and the anti-bonding  $\pi^*$  orbital mainly localized in the five-membered ring. The vertical excitation energy of the  $S_0 \rightarrow S_{N3P}(^1n\pi^*)$  transition is red-shifted from 5.96 eV for the adenine monomer to 5.34 eV for the aqueous  $(dA)_5$ . The initial decay starting from the FC point of  $S_{N3P}(^1n\pi^*)$  is accompanied by an elongation in the C2-N3 bond from 1.328

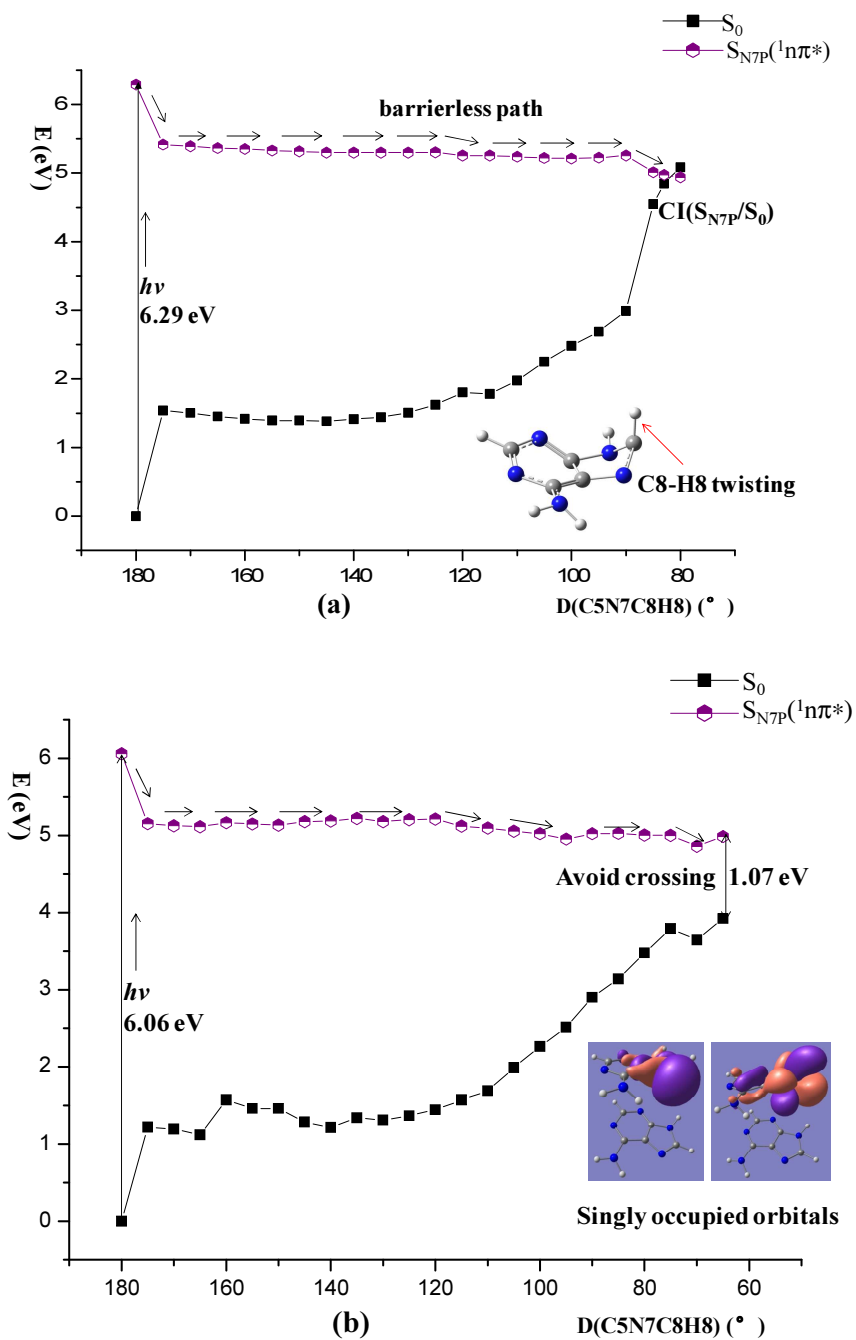


Figure S2. Illustrative relaxation path for the ground state recovery of (a) an adenine monomer in the gas phase; and (b) an aqueous  $(\text{dA})_5$ , starting from the FC point of the  $S_{N7P}(^1n\pi^*)$  state; along the RC defined by the dihedral angle C5N7C8H8.

Å to 1.438 Å with a single bond character at the 175° C4N3C2H2 twisting (see Figure S1). This eliminates the structural constraint for the subsequent C2-H2 bond twisting and decreases the energy by 0.813 and 1.316 eV for the aqueous (dA)<sub>5</sub> and adenine monomer, respectively. As shown in Figure S1 (b), for the adenine monomer the downhill MEP along the C2-H2 bond twisting goes to the conical intersection CI(S<sub>N3P</sub>/S<sub>0</sub>) at a 90° C4N3C2H2 distortion. For the aqueous (dA)<sub>5</sub> a small barrier of 0.13eV is found at a 125~130° C4N3C2H2 dihedral angle along the MEP in the S<sub>N3P</sub>(<sup>1</sup>nπ\*) state. The barrier increases slightly from the adenine monomer to oligomer, which indicates that base stacking interactions exert negligible influence on the S<sub>N3P</sub>(<sup>1</sup>nπ\*) state decay. The route of the S<sub>N3P</sub>(<sup>1</sup>nπ\*) state decay through the structural deformation of the C2-H2 bond twisting is a fast channel for the relaxation of the adenine multimer.

The S<sub>0</sub>→S<sub>N7P</sub>(<sup>1</sup>nπ\*) transition has a higher vertical excitation energy for the isolated adenine (6.29 eV) and aqueous (dA)<sub>5</sub> (6.06 eV) than other two n→π\* transitions. Similar to that in the S<sub>N3P</sub>(<sup>1</sup>nπ\*) state, the initial decay of the S<sub>N7P</sub>(<sup>1</sup>nπ\*) state is characterized by an N7-C8 bond elongation, resulting in a more optimal structure for the C8-H8 bond twisting and a sharp decrease in the potential energy (see Figure S2). The subsequent decay for the isolated adenine is dominated by a barrierless pathway through an energy plateau at ~5.30 eV with respect to the zero level of S<sub>0</sub> along the RC of the C8-H8 bond twisting. Meanwhile, the ground state energy of the adenine monomer rapidly increases from 2.99 eV at 90° to 4.55 eV at 85° C5N7C8H8 distortion, and eventually reaches the conical intersection CI(S<sub>N7P</sub>/S<sub>0</sub>) that lies 4.97 eV above the S<sub>0</sub> minimum. In a similar fashion, the C8-H8 bond twisting of the aqueous (dA)<sub>5</sub> in the S<sub>N7P</sub>(<sup>1</sup>nπ\*) state leads to a flat potential, in which a small barrier (0.10 eV) is



found. However, the decreased C5N7C8H8 angle for (dA)<sub>5</sub> does not result in an energy degeneracy between the S<sub>N7P</sub>(<sup>1</sup>nπ\*) and ground state. The energy gap between these two states of (dA)<sub>5</sub> is 1.07 eV at a 65° C5N7C8H8 distortion, whereas an energy degeneracy is already reached at an 83° C5N7C8H8 angle for the isolated adenine. This indicates that the S<sub>N7P</sub>(<sup>1</sup>nπ\*) state is unlikely involved in the slow ground state recovery for the UV photoexcited adenine multimer.

### Section 3. Computational Details

For the QM/MM interface a hydrogen link-atom scheme was used to saturate the valence of the QM subsystem where the N9-C11 and N9'-C11' bonds were cleaved. To reduce the strong interaction between the two closest MM (C11, C11') point charges and a link atom, these point charges were set to zero.<sup>S3</sup> To compensate for this some point charges of the MM atoms were re-parameterized, where the modified values are summarized in Table S2. The default point charges were used for the remaining MM part. The QM part of the calculation was done at the CASSCF level of theory with the 6-31G\* basis set and an appropriate active space. To describe the  $^1n \rightarrow \pi^*$  transitions originated from the lone pairs of the N1(N1'), N3(N3') and N7(N7') atoms, the corresponding three  $n$  orbitals were included in the active space. Other orbitals came from the  $\pi/\pi^*$  orbitals of the adenine dimer. Since including all of them will be prohibitively expensive, we excluded some unimportant  $\pi$  and  $\pi^*$  orbitals whose occupation numbers are close to 0 or 2. This resulted in a total of 14 active electrons in 10 active orbitals (14e/10o). When searching for the relaxation paths some convergence problems were encountered during the excited state optimizations. This was fixed by excluding the  $n$  orbitals that correspond to the lowest N1 (N1') lone pairs in most cases but are replaced by the N3 (N3') and N7 (N7') lone pairs when the critical points in the  $S_{N3P}$  and  $S_{N7P}$  states were optimized.

**Scheme S1.** Simple diagram of the QM/MM computational protocol for finding the MEPs of the (dA)<sub>5</sub> oligomer: the QM subsystem includes the middle adenine dimer or trimer; other parts of (dA)<sub>5</sub>, the counterions, and a total of 1933 water molecules in the solvent box are treated as the MM part.

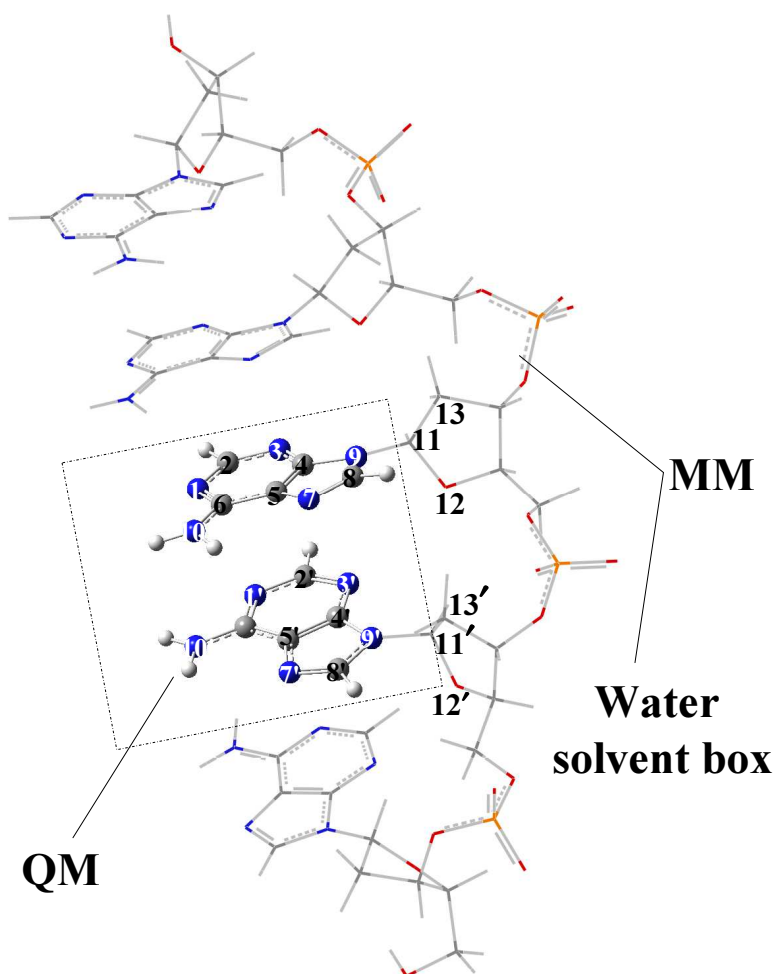


**Table S2.** Re-parameterized point charges in the QM/MM interface region

C11	0.0	C11'	0.0
O12	0.194555	O12'	0.194555
C13	-0.074625	C13'	-0.074625
H11	0.194555	H11'	0.194555

The local minima in different excited states of (dA)<sub>5</sub> were obtained by unconstrained CASSCF/Amber QM/MM optimizations. The constrained energy profiles for relaxation path were obtained using the two root state-averaged CASSCF/Amber stepwise optimizations along the selected RC. These two roots were taken from the ground state and a corresponding excited state with equal weights. For every stationary point optimization, the RC was fixed at given value while other degrees of freedom were totally relaxed without any constraint. The relaxation paths were preliminary mapped along variant value of reaction coordinates. All solvent water molecules with close distance to (dA)<sub>5</sub> and direct mutual interaction are totally relaxed during the CASSCF/Amber QM/MM optimizations. To account for the dynamical correlation effects, single-point energies were recalculated with the corresponding second-order perturbation theory (CASPT2) using a five-root state-averaged CASSCF zeroth-order wave function. The O(1s), N(1s) C(1s), orbitals were frozen in the core and an IPEA-shift value of 0.0 as well as a shift of 0.2 was used in all CASPT2 computations. The vertical excitation energies, the corresponding oscillator strengths, and the transition dipole moments for the

lowest seven excited states of the (dA)<sub>5</sub> oligomer were obtained using the ground state CASSCF(14e/10o) optimizations followed by the seven and eight roots state-averaged CASPT2 and CASSCF state interaction (CASSI) computations. The same computational strategy was used for the calculations of the adenine monomer (9H-adenine). The numbers of roots for the state-averaged CASPT2 calculations were reduced to 6 for the vertical excitation and 4 for the minima, respectively, in the relaxation paths of the adenine monomer. Frequency calculations were carried out to confirm the minima for various excited states of the adenine monomer in vacuo.

The following model procedure was used to define the RC of the relaxation pathway. The QM/MM *unconstrained minimum optimization* of (dA)<sub>5</sub> with all structural parameters relaxation in the S<sub>stack2</sub>(<sup>1</sup>ππ\*), S<sub>N1P</sub>(<sup>1</sup>nπ\*), S<sub>N3P</sub>(<sup>1</sup>nπ\*), S<sub>N7P</sub>(<sup>1</sup>nπ\*), and the inter-base charge transfer S<sub>CT</sub>(<sup>1</sup>ππ\*) states leads to the twisting motion of the C2-H2 bond, the amino group, the C2-H2 bond, the C8-H8 bond, and the C2-H2 bond, respectively. This indicates these twisting motions are responsible for characteristics of structural deformation induced by specific electron transition pattern in the relaxation of corresponding excited states. To describe these twisting motions, C4N3C2H2, C2N1C6N10 and C5N7C8H8 dihedral angles were respectively assigned as the RC for the structural deformation of the C2-H2 bond, amino group and the C8-H8 bond. The same structural deformation in the S<sub>stack2</sub>(<sup>1</sup>ππ\*) state, defined as the “C2 puckering” or “H2 out of plane motion”, was described by changes of the C2N1C4C5 and C6N1C2H2 dihedral angles in the previous literatures.<sup>S4-S6</sup> As discussed in the section of the relaxation of the S<sub>stack2</sub>(<sup>1</sup>ππ\*) state, the different RC choice does not lead to principal discrepancy for the same type of structural deformation.

**References:**

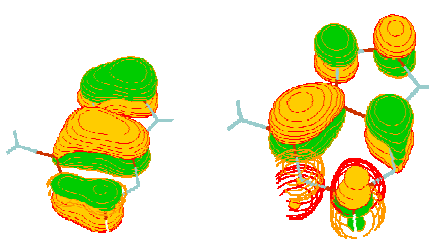
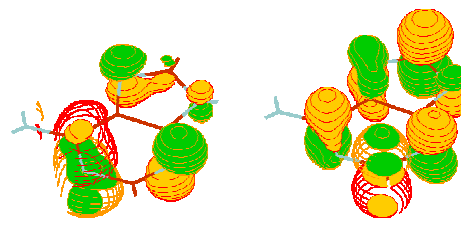
- S1. Y. C. Xu, X. B. Chen, W. H. Fang, D. L. Phillips, *Org. Lett.*, **2011**, *13*, 5472-5475 .
- S2. X. B. Chen, Q. Zhang, Y. C. Xu, D. L. Phillips, *J. Org. Chem.*, **2013**, *78*, 5677–5684.
- S3. N. Ferré, A. Cembran, M. Garavelli, M. Olivucci, *Theo. Chem. Acc.* 2004, **112**, 335-341.
- S4. L. Serrano-Andrés, M. Merchán, A. C. Borin, *Chem. Eur. J.*, 2006, **12**, 6559–6571.
- S5. L. Serrano-Andrés, M. Merchán, A. C. Borin, *Proc. Natl. Acad. Sci. USA*, **2006**, *103*, 8691–8696.
- S6. I. Conti, M. Garavelli, G. Orlandi, *J. Am. Chem. Soc.*, 2009, **131**, 16108–16118.

#### Section 4. Tables

Table S4.1. The absolute energy (A. E.) in Hartree, the oscillator strength ( $f$ ), and the dipole moment in Debye at the Franck-Condon geometry of the adenine monomer in gas phase obtained with the CAS(14, 10)/6-31G\*/CASPT2 level of theory.

	A.E.	$f$	Dipole moment
Root1( $S_0$ )	-465.9372615526		2.4842
Root2( $S_{Lb}({}^1\pi\pi^*)$ )	-465.7556038941	0.45781854E-01	2.3971
Root3( $S_{N1P}({}^1n\pi^*)$ )	-465.7607159931	0.14270935E-02	1.1851
Root4( $S_{N3P}({}^1n\pi^*)$ )	-465.7182253592	0.70721827E-02	0.7449
Root5( $S_{N7P}({}^1n\pi^*)$ )	-465.7059931273	0.15507819E-01	3.0700
Root6( $S_{La}({}^1\pi\pi^*)$ )	-465.7341319513	0.28872498	4.5733

Table S4.2. Assignment of the different transitions at the Franck-Condon geometry of the adenine monomer in gas phase obtained with the CAS(14, 10)/6-31G\*/CASPT2 level of theory.

	Configuration with the largest Coefficient			assignments
<b>Root2</b>	Occupation	Coefficient	Weight	$S_0 \rightarrow S_{LB}(^1\pi\pi^*)$
	22222u20d0	0.52409	0.27467	
	The character of singly occupied orbitals			
				
	Occupation	Coefficient	Weight	
	22u2222d00	0.64631	0.41771	
	The character of singly occupied orbitals			
				



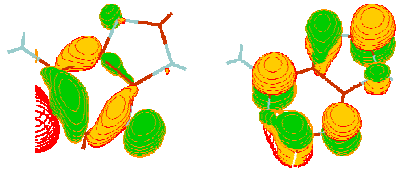
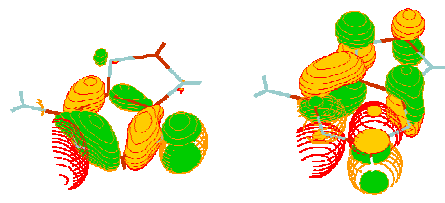
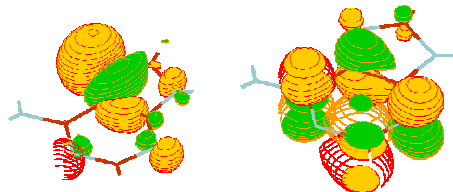
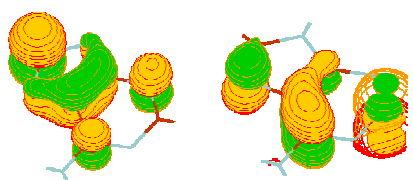
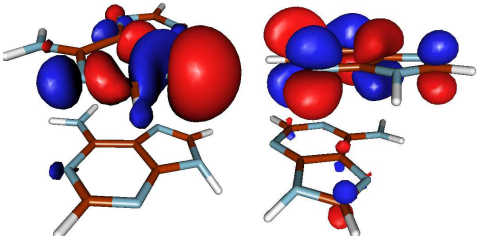
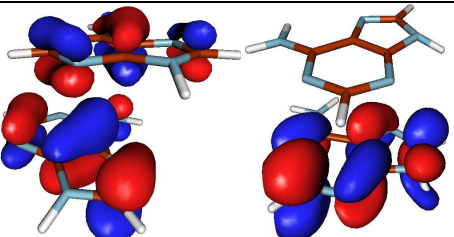
<b>Root3</b>	Occupation	Coefficient	Weight	$S_0 \rightarrow S_{N1}(^1n\pi^*)$
	222222ud00	0.84764	0.71850	
	The character of singly occupied orbitals			
				
<b>Root4</b>	Occupation	Coefficient	Weight	$S_0 \rightarrow S_{N3}(^1n\pi^*)$
	222222u0d0	-0.88663	0.78611	
				
<b>Root5</b>	Occupation	Coefficient	Weight	$S_0 \rightarrow S_{N7}(^1n\pi^*)$
	2222u22d00	0.69832	0.48765	
				
<b>Root6</b>	Occupation	Coefficient	Weight	$S_0 \rightarrow S_{LA}(^1\pi\pi^*)$
	22222u2d00	0.83731	0.70108	
				

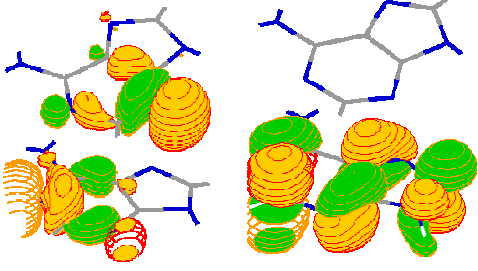
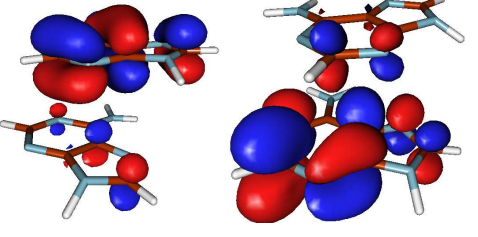
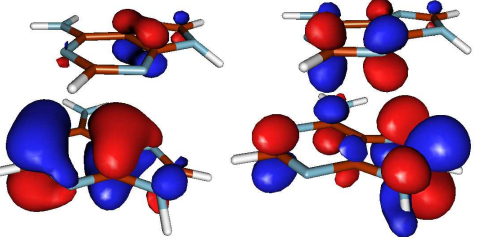
Table S4.4. The absolute energy (A.E.) in Hartree, the energy difference ( $\Delta E$ ) in kcal/mol, the oscillator strength ( $f$ ), and the dipole moment in Debye at the Franck-Condon geometry of the (dA)<sub>5</sub> oligomer in a water solvent calculated using the CAS(14e/10o)/6-31G\*/Amber QM/MM optimizations followed by seven and eight roots state-averaged single point CASPT2(14e/10o) calculations.

	<b>A.E.</b>	$f$	<b><math>\Delta E</math></b>	<b>Dipole moment</b>
root1(S <sub>0</sub> )	-931.8698263006		0.0	4.6019
root2(S <sub>N3P</sub> ( <sup>1</sup> nπ*))	-931.6735643464	0.41092358E-01	123.2	5.3804
root3 (S <sub>stack2</sub> ( <sup>1</sup> ππ*))	-931.6919000786	0.21470301	111.6	5.2820
root4(S <sub>N1P</sub> ( <sup>1</sup> nπ*))	-931.6892066010	0.14026472	113.3	4.8673
Root5(S <sub>Lb</sub> ( <sup>1</sup> ππ*))	-931.6764659862	0.19492281E-01	121.3	4.3301
root6(S <sub>stack1</sub> ( <sup>1</sup> ππ*))	-931.6772904901	0.71393158	120.8	6.9272
Root7(S <sub>CT</sub> ( <sup>1</sup> ππ*))	-931.6377259444	0.11870301E-01	145.6	14.8119

	<b>A.E.</b>	$f$	<b><math>\Delta E</math></b>	<b>Dipole moment</b>
Root1	-931.8700325202			4.2710
Root2	-931.6884083689	0.18606045E-01		4.6050
Root3	-931.6674628335	0.45428499E-04		3.9670
Root4	-931.6684398401	0.11157278E-01		5.7392
Root5(S <sub>N7P</sub> ( <sup>1</sup> nπ*))	-931.6473680200	0.16067944E-01	139.7	3.2698
Root6	-931.6676114427	0.25481418		7.0311
Root7(S <sub>stack1</sub> ( <sup>1</sup> ππ*))	-931.6664768066	0.36871546		8.6820
Root8	-942.2558424217	0.10700074		15.6577

Table S4.5. Assignment of different transitions at the Franck-Condon geometry of the (dA)<sub>5</sub> oligomer in a water solvent box using the CAS(14e/10o)/6-31G\*/Amber QM (dimer)/MM optimizations followed by seven-roots-state-averaged single point CASPT2(14e/10o) calculations.

				Configuration with the largest Coefficient	assignments
Root2	Occupation	Coefficient	Weight		
	22222u20d0	-0.58985	0.34793		
	The character of singly occupied orbitals				
					$S_0 \rightarrow S_{N3P}(^1n\pi^*)$
				Configuration with the largest Coefficient	
Root3	Occupation	Coefficient	Weight		
	222u222d00	0.49460	0.24463		
	The character of singly occupied orbitals				
					$S_0 \rightarrow S_{Stack2}(^1\pi\pi^*)$

				<b>Configuration with the largest Coefficient</b>			
<b>Root4</b>	Occupation	Coefficient	Weight				$S_0 \rightarrow S_{NIP}(^1n\pi^*)$
	22222u2d00	0.52123	0.27168				
	The character of singly occupied orbitals						
							
<b>Root5</b>	Occupation	Coefficient	Weight				$S_0 \rightarrow S_{LB}(^1\pi\pi^*)$
	222u22200d	-0.50566	0.25569				
	The character of singly occupied orbitals						
							
	Occupation	Coefficient	Weight				
	u222222d00	-0.43109	0.18584				
The character of singly occupied orbitals							
							

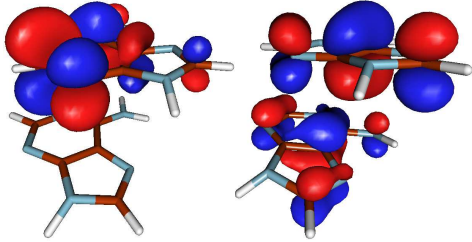
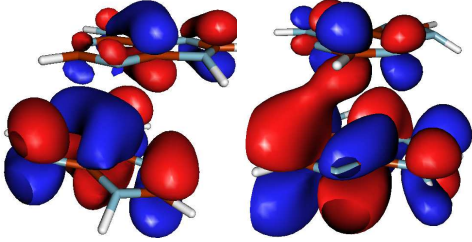
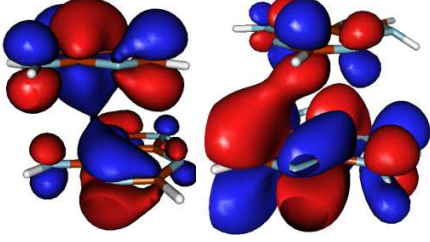
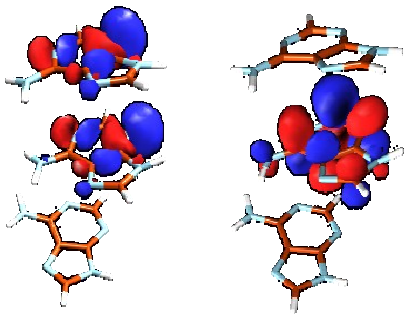
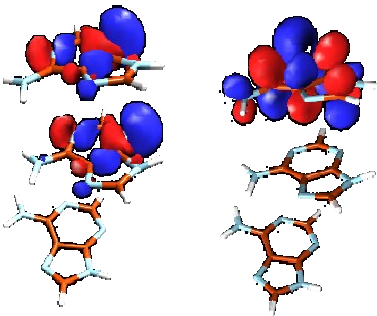
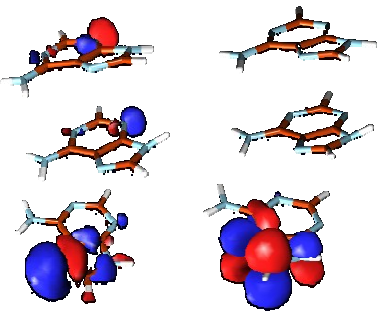
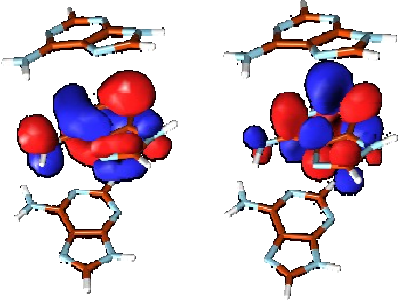
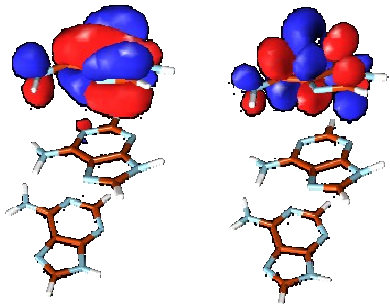
Configuration with the largest Coefficient				
<b>Root6</b>	Occupation	Coefficient	Weight	$S_0 \rightarrow S_{\text{Stack1}}(^1\pi\pi^*)$
	2222u220d0	-0.71341	0.50895	
	The character of singly occupied orbitals			
				
<b>Root7</b>	Occupation	Coefficient	Weight	$S_0 \rightarrow S_{\text{CT}}(^1\pi\pi^*)$
	2222u22d00	0.69944	0.48922	
				
	Occupation	Coefficient	Weight	
	222u222d00	0.57767	0.33370	
				

Table S4.6. Assignment of different transitions at the Franck-Condon geometry of the (dA)<sub>5</sub> oligomer in a water solvent box using the CAS(14e/10o)/6-31G/Amber QM (trimer)/MM optimizations followed by seven-roots-state-averaged single point CASPT2(14e/10o) calculations.

		<b>Configuration with the largest Coefficient</b>			<b>assignments</b>
<b>Root2</b>	Occupation	Coefficient	Weight		<b>S<sub>0</sub>→S<sub>NP</sub>(<sup>1</sup>nπ*)</b>
	22222u2d00	-0.68305	0.46655		
	The character of singly occupied orbitals				
					
		<b>Configuration with the largest Coefficient</b>			
<b>Root3</b>	Occupation	Coefficient	Weight		<b>S<sub>0</sub>→S<sub>NP</sub>(<sup>1</sup>nπ*)</b>
	22222u200d	-0.64337	0.41393		
	The character of singly occupied orbitals				

				
	<b>Configuration with the largest Coefficient</b>			<b>assignments</b>
<b>Root4</b>	Occupation	Coefficient	Weight	$S_0 \rightarrow S_{N1P}(^1n\pi^*)$
	2222u220d0	-0.87008	0.75704	
	The character of singly occupied orbitals			
				
	<b>Configuration with the largest Coefficient</b>			
	Occupation	Coefficient	Weight	
	2u22222d00	0.80317	0.64508	
	The character of singly occupied orbitals			

<b>Root5</b>				$S_0 \rightarrow S_{\text{stack}2}({}^1\pi\pi^*)$
	<b>Configuration with the largest Coefficient</b>			
	Occupation	Coefficient	Weight	
	222u22200d	-0.82423	0.67936	
	The character of singly occupied orbitals			
<b>Root6</b>				$S_0 \rightarrow S_{\text{stack}1}({}^1\pi\pi^*)$
	<b>Configuration with the largest Coefficient</b>			<b>assignments</b>
	Occupation	Coefficient	Weight	
	222u222d00	0.95943	0.92050	
	The character of singly occupied orbitals			



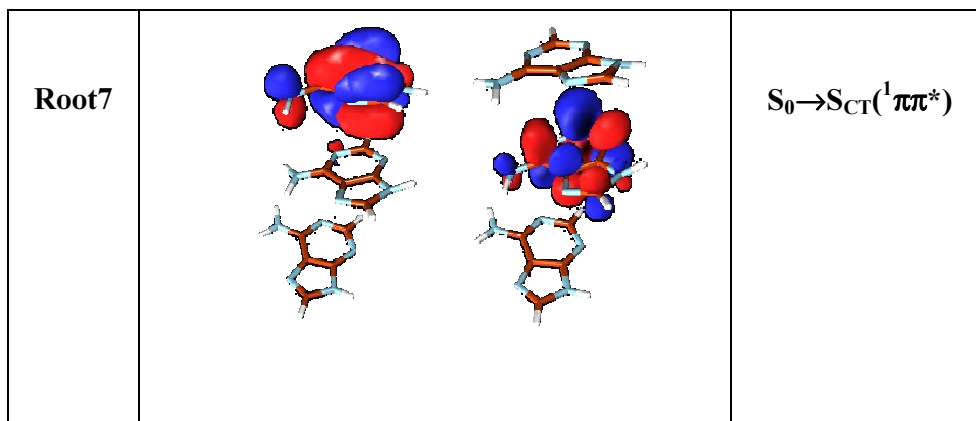


Table S4.7. The charge translocation ( $\Delta q$ ) between the five- and six-membered rings of adenine dimer for the  $S_0 \rightarrow S_{stack1}(^1\pi\pi^*)$  and  $S_0 \rightarrow S_{stack2}(^1\pi\pi^*)$  transitions versus the translational distance [ $\delta$  (T. D.)] in Å with respect to the ground state ( $S_0$ ) equilibrium value of the aqueous  $d(A)_5$  at the CASPT2//CASSCF(14e/10o) level of theory.

$\delta$ (T. D.)	Transitions	$\Delta q_{v_i-v}$	$\Delta q_{v_i'-v'}$
	$S_0$	-0.421	-0.471
0	$S_0 \rightarrow S_{\text{stack1}}(^1\pi\pi^*)$	-0.938	-0.413
	$S_0 \rightarrow S_{\text{stack2}}(^1\pi\pi^*)$	-0.427	-0.231
	$S_0$	-0.420	-0.471
0.310	$S_0 \rightarrow S_{\text{stack1}}(^1\pi\pi^*)$	-0.928	-0.413
	$S_0 \rightarrow S_{\text{stack2}}(^1\pi\pi^*)$	-0.422	-0.230
	$S_0$	-0.417	-0.471
0.637	$S_0 \rightarrow S_{\text{stack1}}(^1\pi\pi^*)$	-0.898	-0.410
	$S_0 \rightarrow S_{\text{stack2}}(^1\pi\pi^*)$	-0.421	-0.260
	$S_0$	-0.417	-0.472
0.670	$S_0 \rightarrow S_{\text{stack1}}(^1\pi\pi^*)$	-0.888	-0.404
	$S_0 \rightarrow S_{\text{stack2}}(^1\pi\pi^*)$	-0.423	-0.277
	$S_0$	-0.419	-0.437
0.693	$S_0 \rightarrow S_{\text{stack1}}(^1\pi\pi^*)$	-1.068	-0.430
	$S_0 \rightarrow S_{\text{stack2}}(^1\pi\pi^*)$	-0.407	-0.871
	$S_0$	-0.446	-0.465
0.753	$S_0 \rightarrow S_{\text{stack1}}(^1\pi\pi^*)$	--	--
	$S_0 \rightarrow S_{\text{stack2}}(^1\pi\pi^*)$	-0.439	-0.924
	$S_0$	-0.448	-0.472
0.893	$S_0 \rightarrow S_{\text{stack1}}(^1\pi\pi^*)$	--	--
	$S_0 \rightarrow S_{\text{stack2}}(^1\pi\pi^*)$	-0.440	-0.936

## **Section 5, Energy tables and Cartesian coordinates of the optimized structures**

In this work, we optimized too many structures in various electronic states. If all Cartesian coordinates and relative energies are given in this supplementary information, the file will be very long. As an alternative solution, we made a separated file with all cartesian coordinates and tables with all relative energies for the optimized structures that is available through email [xuebochen@bnu.edu.cn](mailto:xuebochen@bnu.edu.cn) from Xuebo Chen upon request.